

Enhanced Tumor Uptake and Penetration of Virotherapy Using Polymer Stealthing and Focused Ultrasound

Robert Carlisle, James Choi, Miriam Bazan-Peregrino, Richard Laga, Vladimir Subr, Libor Kostka, Karel Ulbrich, Constantin-C. Coussios, Leonard W. Seymour

Manuscript received April 16, 2013; revised September 5, 2013; accepted September 20, 2013.

Correspondence to: Dr Robert Carlisle, University of Oxford, Institute of Biomedical Engineering, Old Raod Campus, Headington, Oxford, Oxon OX3 7DQ, UK (e-mail: robert.carlisle@eng.ox.ac.uk).

- Background** Oncolytic viruses are among the most powerful and selective cancer therapeutics under development and are showing robust activity in clinical trials, particularly when administered directly into tumor nodules. However, their intravenous administration to treat metastatic disease has been stymied by unfavorable pharmacokinetics and inefficient accumulation in and penetration through tumors.
- Methods** Adenovirus (Ad) was “stealthed” with a new *N*-(2-hydroxypropyl)methacrylamide polymer, and circulation kinetics were characterized in Balb/C SCID mice ($n = 8$ per group) bearing human ZR-75-1 xenograft tumors. Then, to noninvasively increase extravasation of the circulating polymer-coated Ad into the tumor, it was coinjected with gas microbubbles and the tumor was exposed to 0.5 MHz focused ultrasound at peak rarefactional pressure of 1.2 MPa. These ultrasound exposure conditions were designed to trigger inertial cavitation, an acoustic phenomenon that produces shock waves and can be remotely monitored in real-time. Groups were compared with Student *t* test or one-way analysis of variance with Tukey correction where groups were greater than two. All statistical tests were two-sided.
- Results** Polymer-coating of Ad reduced hepatic sequestration, infection (>8000 -fold; $P < .001$), and toxicity and improved circulation half-life (>50 -fold; $P = .001$). Combination of polymer-coated Ad, gas bubbles, and focused ultrasound enhanced tumor infection >30 -fold; (4×10^6 photons/sec/cm²; standard deviation = 3×10^6 with ultrasound vs 1.3×10^5 ; standard deviation = 1×10^5 without ultrasound; $P = .03$) and penetration, enabling kill of cells more than 100 microns from the nearest blood vessel. This led to substantial and statistically significant retardation of tumor growth and increased survival.
- Conclusions** Combining drug stealthing and ultrasound-induced cavitation may ultimately enhance the efficacy of a range of powerful therapeutics, thereby improving the treatment of metastatic cancer.
- J Natl Cancer Inst;2013;105:1701–1710

Oncolytic adenoviruses (Ads) selectively replicate within and destroy cancer cells, making them one of the most powerful therapeutics available. However, all robust responses reported to date (1–3) have relied on intratumoral injection, and until Ads can achieve efficacy following intravenous delivery their clinical use will be restricted. In particular, systemic delivery of Ads to treat metastatic cancer will require improved circulation kinetics, extravasation from the bloodstream into the tumor, and intratumoral penetration.

After intravenous delivery, Ads bind antibodies, complement, and blood cells (4,5). In response, “stealthing” technologies have been developed, whereby Ads are coated with biocompatible polymers such as polyethylene glycol or *N*-(2-hydroxypropyl)methacrylamide (6–9). Stealthing removes natural Ad tropism and prevents binding to blood components, leading to extended circulation (10). However, by stealthing Ads to provide sufficient protection during delivery, their ability to infect cells upon arrival

in tumors is often compromised. To meet this challenge, polymers can be designed to selectively degrade upon exposure to the tumor milieu. This is possible because dysregulated growth of cells within tumors creates a hypoxic and low pH environment that is distinct from normal tissue (11,12). We report the development of a coating polymer that enhances circulation and also allows triggered uncoating and reactivation of Ads within tumors.

Despite benefiting from the enhanced permeability retention effect (13), the passage of stealthed Ads from the bloodstream into tumors is still suboptimal, with less than 0.1% of dose achieving deposition in the tumor (4). Furthermore, the intratumoral distribution of Ads remains exclusively perivascular, and without penetration deep into the tumor, the therapeutic effect is restricted to a small proportion of its mass. Such limitations are shared by other therapeutics, such as drug–polymer conjugates and liposomes (14–17). In response, external stimuli have been applied to improve uptake

into and spread through tumors (18–21). We feel that focused ultrasound is the safest and most clinically applicable of these strategies. Indeed, our *in vitro* studies have shown that ultrasound can provide a powerful stimulus to propel Ads deep into tumor-mimicking material (22). To achieve these effects, Ads were coadministered with a microbubble formulation (SonoVue [SV]), which provided nuclei for the initiation of a phenomenon known as inertial cavitation. This term describes the expansion, contraction, and violent collapse of a bubble in response to ultrasound, which creates microstreaming and shock waves. Such events can be used to move macromolecules more than 200 μm (21). The use of microbubbles and ultrasound to improve Ad delivery to tumors is ideal because the ultrasound pressures required are modest and clinically applicable and the inertial cavitation events created are targetable and produce distinct nonharmonic emissions that can be mapped, providing valuable feedback on the success of the procedure (23).

We have improved the efficacy of Ads by combining stealthing and ultrasound to overcome their poor pharmacokinetics and limited extravasation and penetration into the tumor.

Methods

Cells and Ads

Human breast cancer cell line ZR-75-1 from ATCC (<http://www.lgcstandards-atcc.org>) was grown and cultured in accordance with instructions and was used within 10 passages of purchase. Nonreplication competent AdLuc and AdGFP were from NAC (Oxford, UK). Oncolytic AdEHE2F-luc was grown, as previously described (24).

Level Low pH Labile Hydrazone Bond-Containing Copolymer-Monomer Synthesis

2-Methyl-*N*-[5-[1-methyl-6-oxo-6-(2-thioxo-thiazolidin-3-yl)-hexylidene-hydrazinocarbonyl]-pentyl]-acrylamide (Ma-AH-NHN=OH-TT) was prepared by a two-step procedure: Ma-AH-NHNH₂ (0.15 g, 0.703 mmol) was dissolved in methanol dried with calcium hydride (1 mL), and 6-oxoheptanoic acid dried over phosphorous pentoxide was added (0.113 g, 0.780 mmol) in the presence of 4-(1,1,3,3-tetramethylbutyl)pyrocatechol as inhibitor. The reaction was catalyzed by addition of acetic acid (5 μL) for 2 hours at room temperature. Methanol was evaporated, and the oily residue was dried for 1 hour on vacuum. Oily residue was dissolved in dichloromethane (2 mL), and 4,5-dihydrothiazole-2-thiol (0.093 g, 0.780 mmol) was added, followed by *N*-(3-dimethylaminopropyl)-*N'*-ethylcarbodiimide hydrochloride (DMAEC·HCl) (0.180 g, 0.94 mmol) and catalytic amount of 4-dimethylaminopyridine. Reaction mixture was stirred (3 hours at room temperature), then diluted with dichloromethane (10 mL) and extracted three times with sodium bicarbonate solution (2 wt%, 10 mL). The organic layer was separated and dried with a sodium sulfate. The dichloromethane was evaporated in a vacuum, and the oily residue was dissolved in dried methanol (2 mL) and purified on a Sephadex LH-20 column (GE Healthcare, Amersham, UK) in methanol. The methanol was evaporated, and the oily product was dried on vacuum and stored at -18°C . Yield was 0.123 g (54%).

Low pH Labile Hydrazone Bond-Containing Copolymer-Polymer Synthesis

Multivalent reactive hydrazone copolymer poly(HPMA-co-Ma-AH-NHN=OH-TT) was prepared by solution radical copolymerization of HPMA (25) (0.25 g, 1.75 mmol) and Ma-AH-NHN=OH-TT (0.085 g, 0.19 mmol) in dimethyl sulfoxide (1.87 mL) initiated with azobisisobutyronitrile (0.034 g; 60°C for 6 hours). Polymer was isolated by precipitation into a mixture of acetone and diethylether (2:1), filtered off, washed with acetone and diethylether, dried in vacuum, and characterized by size exclusion chromatography (SEC). Yield was 0.265 g. Content of TT groups was 5.5 mol%, with a weight average mass (M_w) of 37 500 and molar mass dispersity (\mathcal{D}_M) of 1.95.

Pharmacokinetics, Organ Accumulation, and Focused Ultrasound Application

UK Home Office guidelines and the UKCCCR Guidelines for the Welfare of Animals in Experimental Neoplasia were followed. ZR-75-1 human breast carcinoma cells (5×10^6) were implanted into BalbC/SCID mice (Harlan, UK) in one site (survival studies) or into each hind leg (accumulation studies). Mice were given 5 $\mu\text{g}/\text{mL}$ of 17 β -estradiol (Sigma, St Louis, USA) in drinking water. After 4 to 6 weeks, clodronate liposomes (150 $\mu\text{L}/\text{mouse}$, www.clodronateliposomes.com) were injected. Twenty-four hours later, mice were randomized ($n = 8$ per group) and injected with 1×10^{10} Ad or polymer coated Ad (PC-Ad) in 50 μL of phosphate-buffered saline (PBS) mixed with 50 μL of SV (Bracco, Italy). Dose was fractionated in two, with 50 μL injected at 0 minutes and 50 μL injected 2 minutes later (to ensure sustained blood SV concentrations).

Ultrasound was applied to the tumor using the chamber and equipment represented in [Supplementary Fig. 2, A](#) (available online) to deliver the following ultrasound parameters - frequency: 0.5 MHz, pulse length: 50 000 cycles, pulse repetition frequency: 0.5 Hz, peak rarefactional pressure: 1.2 MPa for 4 minutes after Ad or PC-Ad injection. Control mice were placed in the chamber but ultrasound was not applied. Blood samples taken at 5, 15, and 30 minutes after injection were analyzed for Ad content by quantitative polymerase chain reaction (QPCR) [see (10)]. In distribution studies, mice were killed by cervical dislocation at 24 hours and livers and tumors were harvested and Ad genome content was calculated [see (10)]. Images were captured using an IVIS 100 system (Xenogen, Hopkinton, MA, USA). Tumors were measured using callipers and the formula (height \times width \times diameter)/2, growth was plotted. Starting size averaged 98 mm³ (standard deviation [SD] = 25) for PBS, 107 mm³ (SD = 32) for SV + ultrasound, 91 mm³ (SD = 30) for PC-Ad + SV, and 101 mm³ (SD = 25) for PC-Ad + SV + ultrasound. Alanine transaminase (ALT) levels were assayed by taking and analyzing plasma 24 hours after dosing with Ad or PC-Ad using a Bioo Scientific kit (Austin, TX, USA) according to the manufacturer's instructions, using the standard provided in the kit to produce a line with an R^2 value of 0.985.

Statistical Analysis

Testing was performed using Prism 5 graph pad (<http://www.graphpad.com/scientific-software/prism/>) software. Statistical significance ($***P < .001$, all other P values as stated) was calculated using Student t test in cases of two comparison groups and one-way

analysis of variance (ANOVA) with Tukeys correction in cases of more than two comparison groups. All statistical tests were two-sided. Standard deviations are given. Log-rank testing was used to analyze survival data, and area under the curve was calculated as the mean value of the summed individual areas for all mice in each group.

Results

Polymer Coating for Protection and Low pH Triggered Reactivation of Ad

Tumor accumulation of intravenous Ad is limited by binding to antibodies, complement, and blood cells and rapid capture by the reticuloendothelial system (4–6,10). Polymer coating can provide protection against such binding/capture but often also compromises Ad tumor infectivity (8). To achieve protection while

maintaining infectivity, we synthesised an *N*-(2-hydroxypropyl) methacrylamide copolymer, (Supplementary Figure 1A, available online), containing hydrazone bonds, designed to undergo uncoating of Ad upon exposure to low pH.

Coating of Ad with copolymer, to give PC-Ad (or nondegradable control copolymer, to give ND PC-Ad), produced monodisperse populations of 130-nm particles (Supplementary Figure 1B, available online). Enzyme-linked immunosorbent assay demonstrated that binding of anti-Ad antibodies was inhibited for both PC-Ad (absorbance = 0.157; SD = 0.06) and ND PC-Ad (absorbance = 0.163; SD = 0.01) compared with Ad (absorbance = 0.429; SD = 0.019; $P < .001$) (Figure 1A), indicating that inclusion of low pH cleavable bonds in the copolymer structure does not reduce coating and protection of Ad. When this assay was performed after exposure of PC-Ad to low pH, complete restoration of antibody binding was observed, indicative of triggered

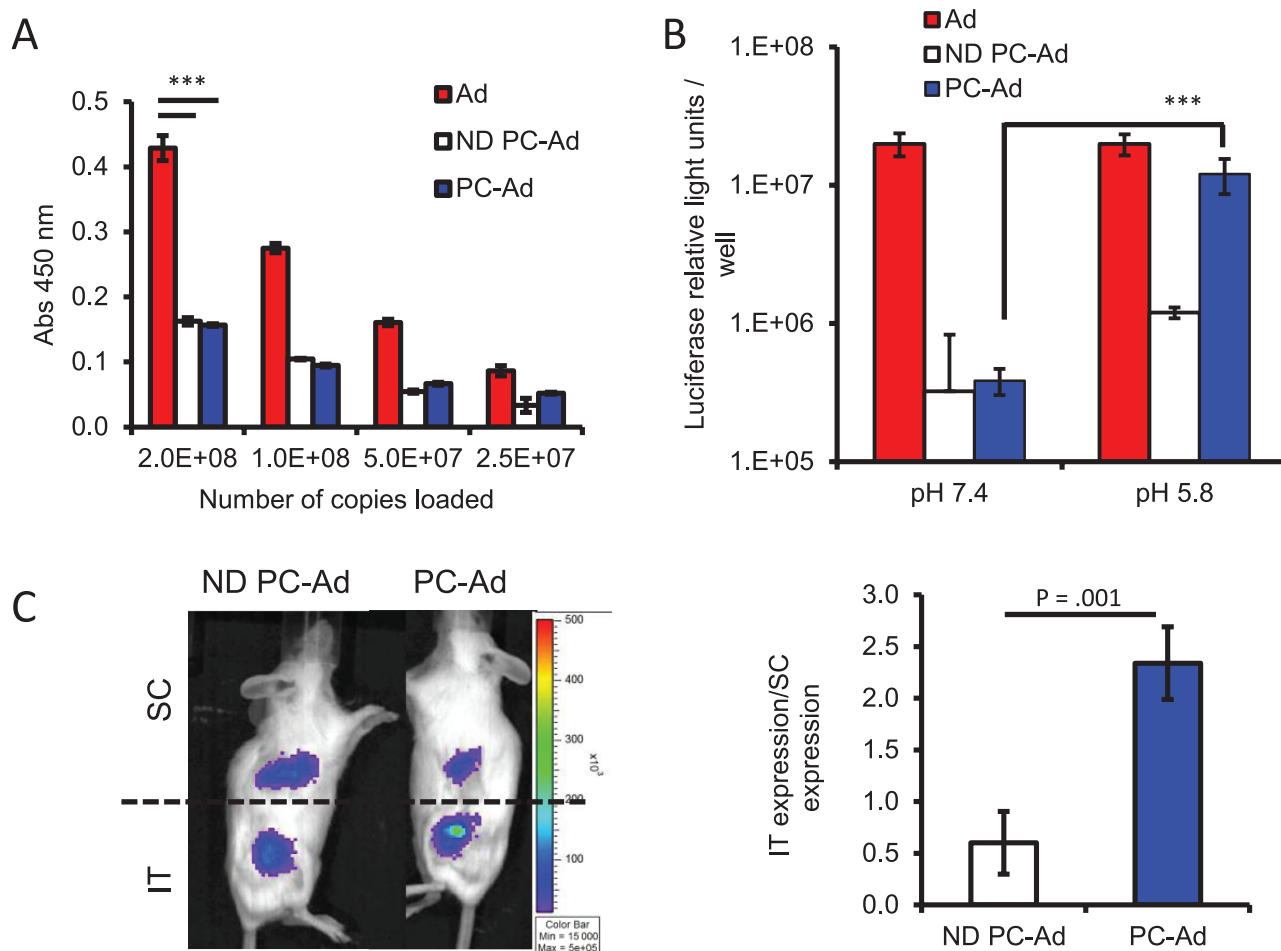


Figure 1. Testing efficiency and reversibility of Adenovirus (Ad) polymer coating. **A** After stealthing with nondegradable (ND PC-Ad) or low pH labile (PC-Ad) polymer, Ad shows reduced binding to enzyme-linked immunosorbent plates coated with antiadenovirus antibody, indicating effective protection of the Ad by stealthing with polymer. **B** In vitro characterization of low pH triggered uncoating of PC-Ad by infection of a ZR-75-1 monolayer after pre-incubation of Ad, ND PC-Ad, or PC-Ad at pH 7.4 or 5.8. PC-Ad stealths Ad to effectively inhibit infection at pH 7.4 but stealthing is reversed and infection restored as pH is lowered. **C** In vivo assessment of triggered uncoating after direct injection of 20 μ L/5 $\times 10^8$ particles of ND PC-Ad (right flank) or PC-Ad (left flank)

subcutaneously (SC) or into ZR-75-1 xenograft tumors. Measurement of luciferase transgene expression 24 hours later by IVIS. The image shows a representative mouse. The graph shows data from all three mice calculated as a ratio of intratumoral (IT) expression level divided by expression level after SC injection. Higher expression in tumors injected with PC-Ad indicates utility of pH triggered de-stealth and infection reactivation in vivo. In the graph in (C), $n = 3$ mice; standard deviation (SD) is shown by bars. In other parts, $n = 4$; SD is shown by bars. *** $P < .001$, analysis using *t* test (C) or analysis of variance (A and B). Results typical of 3 independent experiments. All statistical tests were two-sided.

uncoating (Supplementary Figure 1C, available online). Coating of the capsid epitopes of Ad responsible for binding to receptors on cancer cells reduced the infectivity of PC-Ad 100-fold. However, infection was restored by preincubation of PC-Ad at low pH, confirming triggered uncoating. Levels of luciferase were 30-fold higher with PC-Ad at pH 5.8 ($>1.2 \times 10^7$ light units per well; SD = 1.2×10^6) compared to PC-Ad at pH 7.4 ($<4 \times 10^5$; SD = 8×10^4 ; $P < .001$) (Figure 1B).

To test pH response in vivo, subcutaneous and intratumoral injection of Adluc was performed. Mice receiving PC-Adluc had greater than twofold higher luciferase levels at the intratumoral site than the subcutaneous site, whereas mice receiving ND PC-Adluc had higher levels at the subcutaneous site than the intratumoral site ($P = .001$) (Figure 1C). This indicates tumor-selective reactivation of the PC-Adluc, commensurate with activation by intratumoral pH, and establishes the suitability of this vector platform for studies using ultrasound to enhance tumor delivery.

Resistance of Polymer-Coated Ad to the Binding of Human Blood Components

Bloodstream compatibility of PC-Ad was assessed ex vivo using human blood components. The dramatic differences between human and murine Ad clearance mechanisms (4–6,26) mean that the success and utility of polymer coating can not be judged without such studies.

Release of complement protein C3a relates stoichiometrically to C3b deposition on antigen surface, which mediates binding to blood cells and RES clearance (27). Incubation of Ad with plasma resulted in approximately 10-fold more ($P < .001$) C3a release than after incubation with PC-Ad (Figure 2A), indicating that coating Ad may lower complement- and blood cell-mediated clearance (4). Indeed, upon mixing with whole blood, approximately 90% of PC-Ad associated with the plasma fraction, whereas Ad was exclusively recovered from the cell fraction ($P = .003$) (Figure 2B). Coating also inhibited infection of human leukocytes, both in

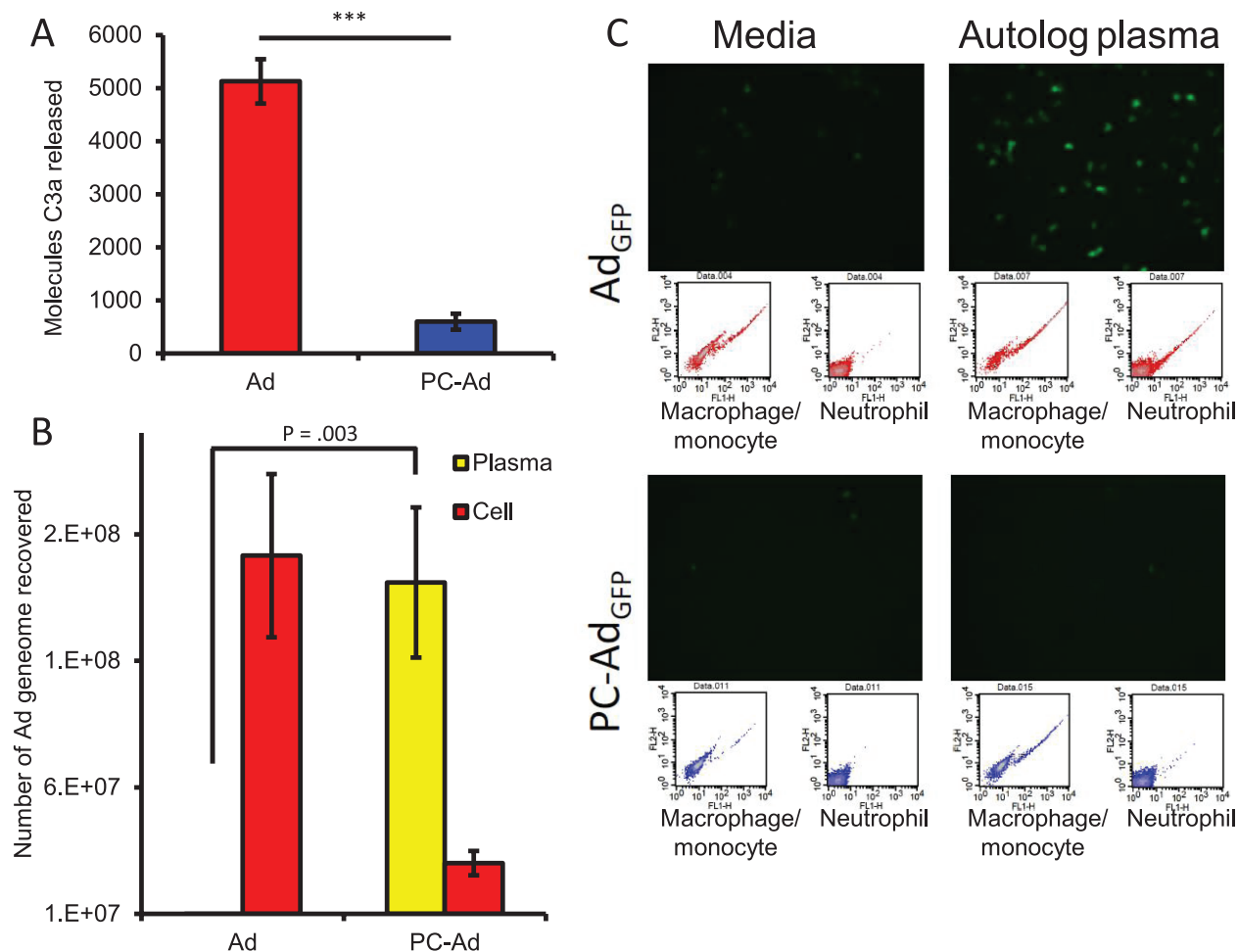


Figure 2. Influence of polymer coating on interaction with bloodstream components. **A**) The effect of polymer coating on complement activation as assayed by C3a release after incubation with fresh human plasma for 30 minutes at 37°C. Reduced complement activation will lower immunogenicity and complement mediated clearance. **B**) The influence of polymer coating on sequestration by human blood cells by assessment of the association with cell and plasma fractions after 30 minutes at 37°C, using quantitative polymerase chain reaction to detect adenovirus (Ad) genomes. Reduced blood cell binding

will extend the circulation of polymer coated Ad (PC-Ad) in vivo. **C**) Characterization of the effect of polymer coating on leukocyte infection using Ad_{GFP} and flow cytometry for detection of cells expressing the green fluorescent protein (GFP) transgene. Lower leukocyte infection will lower immunogenicity and enhance safety. All panels, $n = 3$. Standard deviation is shown by bars. *** $P < .001$, analysis using t test (**A**) or analysis of variance with Tukey post test (**B**). Results typical of 3 experiments. All statistical tests were two-sided. White bar in (**C**) represents 10 microns.

media and in neat autologous plasma (Figure 2C; Supplementary Figure 1D, available online). In accordance with previous findings (5,28,29), monocyte/macrophage and neutrophil populations were infected by Ad, emphasizing the improved safety profile of PC-Ad.

Influence of Polymer Coating and Ultrasound on Circulation Kinetics and Tumor Uptake

Having established the benefit of degradable vs nondegradable polymer coating of Ad *in vitro*, *ex vivo*, and within directly injected tumors, the pharmacokinetics, liver capture, and tumor accumulation of PC-Ad were tested in BalbC/SCID mice bearing ZR-75-1 xenografts. To assess whether ultrasound could be used as a stimulus to drive circulating Ad or PC-Ad from the bloodstream into the tumor, virus was coinjected with the microbubble formulation SV and ultrasound was applied to the tumor. SV microbubbles expand and collapse in response to ultrasound, creating inertial cavitation (30). The oncolytic AdEHE2F-luc encoded luciferase, allowing measurement of virus infection (24).

Polymer coating of Ad improved circulation half-life (>50-fold; $P = .001$). Ad clearance was rapid, with less than 0.5% of the dose still circulating at 30 minutes, whereas PC-Ad showed extended circulation, with more than 30% in the bloodstream at 30 minutes (Figure 3A). These levels are similar to those previously reported using Ad and nondegradable polymer (10). The ability of ultrasound + SV to instigate cavitation activity within the tumor was confirmed by measurement of radiated acoustic emissions, which were passively detected using a single-element focused transducer, thereby allowing monitoring of the presence, type, and magnitude of cavitation at the ultrasound focus (see Supplementary Figure 2A, available online). The application of ultrasound in the absence of SV produced no cavitation signal (data not shown), whereas ultrasound exposure combined with intravenous injection of SV always produced acoustic emissions characteristic of cavitation activity within the tumor (Supplementary Figure 2B, available online). Frequency spectra detected over the duration of the treatment (Supplementary Figure 2C, available online) showed emissions coincident with SV administration and spanning a wide frequency range, demonstrating the presence of the broadband emissions. Such emissions are produced by expansion and violent collapse of the SV and prove the occurrence of inertial cavitation. We have shown previously that such cavitation events assist the movement of Ad *in vitro* (22).

Infection levels were tracked by IVIS imaging of luciferase (Figure 3B). Twenty hours after injection, the signal from livers of Ad-treated mice was off-scale, whereas PC-Ad mice showed comparatively minimal expression. Post-cull *in vitro* analysis of livers showed greater than 8000-fold ($P < .001$) lower luciferase in PC-Ad mice (Supplementary Figure 2D, available online). In separate experiments, PC-Ad caused no increase in hepatic damage. In contrast, in Ad-treated mice, hepatic infection proved to be highly toxic with raised serum ALT levels (230 IU/L) (Figure 3C), requiring the mice be killed. This toxicity had prevented analysis of long-term tumor growth response in our previous studies using Ad + ultrasound (31) and emphasizes the crucial role of polymer coating in improving the clinical applicability of this approach.

To assess the influence of polymer coating and ultrasound on bio-distribution, virus + SV was injected intravenously into mice bearing a tumor on each hind leg, one of which was exposed to ultrasound,

the other of which was not. Analysis (Figure 3D) demonstrated that, in accordance with the high hepatic infection and toxicity observed in Ad mice (Figure 3, B and C), more than 80% of Ad was liver associated. Furthermore, ultrasound + SV gave no increase in the number of Ad in tumors, with just 0.08% of dose accumulating with or without ultrasound + SV, in accordance with previous studies (31). In contrast PC-Ad showed minimal liver capture (<3%), again emphasising its improved safety and circulation profile. Notably, in accordance with previous studies (32), the increased area under the curve (Supplementary Figure 2E, available online) provided by evasion of liver capture allowed enhanced PC-Ad uptake into tumors. Furthermore, an additional twofold ($P = .03$) increase in tumor accumulation of PC-Ad resulted from SV + ultrasound exposure, enabling 0.33% of PC-Ad dose to accumulate (Figure 3E).

Combining polymer coating to enhance bloodstream concentrations and ultrasound to move these enhanced concentrations into the tumor provided levels of virus that we have never previously achieved within this tumor model. This gave a liver/tumor Ad ratio of less than 8:1 for PC-Ad compared with greater than 1000:1 for Ad. This is the first demonstration that ultrasound can enhance the number of virus particles achieving tumor uptake. The failure to achieve an increase in the total number of nonmodified Ads entering tumors in response to ultrasound in these and our previous studies (31) may result from the poor circulation kinetics of Ads. Such poor circulation provides an Ad dose in the tumor vasculature that is not consistently high enough to enable ultrasound exposure to impact on its transfer into tumors in an effective and reliable way. In contrast, polymer coating provides sustained high bloodstream doses, allowing the impact of ultrasound exposure to be fully realized.

Influence of Ultrasound on Penetration and Antitumor Efficacy of PC-Ad

Experiments were performed to assess whether enhanced PC-Ad accumulation in tumors could lead to improved antitumor activity.

Mice bearing one ZR-75-1 tumor were injected intravenously with PC-Ad + SV, with or without the application of ultrasound. The replication and lytic spread of Ad was tracked by measurement of luciferase and daily tumor sizing. After 20 hours, luciferase expression in tumors of ultrasound-treated mice exceeded the level in non-ultrasound-treated mice by threefold ($P = .007$). This enhancement level may be below the level seen in some mice in our previous studies using nonmodified Ad (31), but its dramatically reduced variability provides a substantial benefit. Furthermore, it is notable that this differential increased to 20-fold by 2 days ($P = .004$) and 30-fold by 3 days (4×10^6 light units; SD = 3×10^6 for PC-Ad+SV+ultrasound group vs 1.3×10^5 ; SD = 1×10^5 for PC-Ad+SV group; $P = .03$) (Figure 4A). In ultrasound-treated mice, substantial luciferase was detected in every tumor by day 3. These levels were not matched in non-ultrasound-treated mice until day 21, and even then expression was not observed in tumors of all mice (Supplementary Figure 3, B and C, available online). These dramatic increases in virus activity indicate that ultrasound may enhance penetration of PC-Ad into tumors, whereupon improved access to a low pH and hypoxic environment (33), which is more supportive of copolymer uncoating and virus replication (24), enhances infection. In total, ultrasound provided a

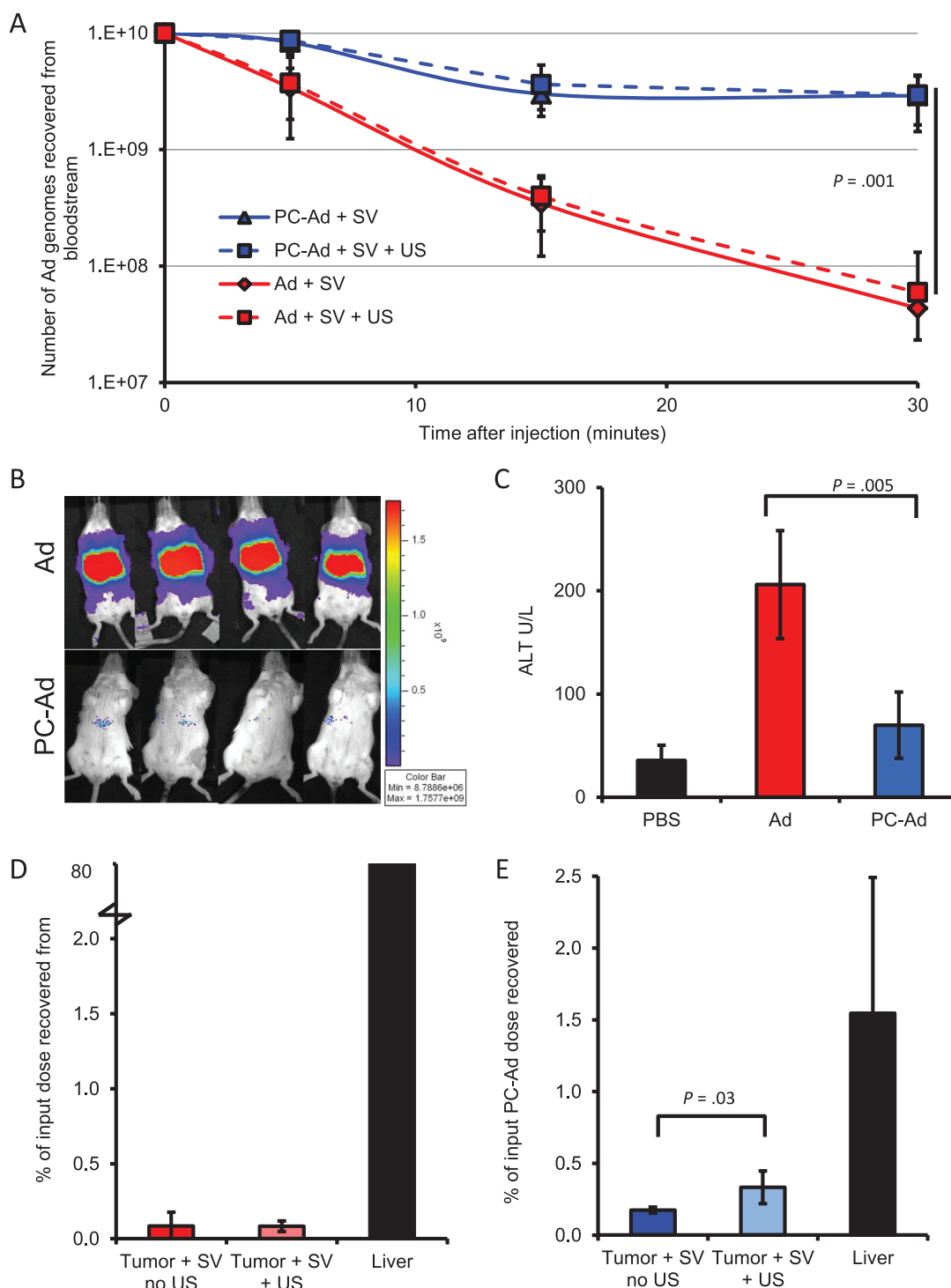


Figure 3. Impact of SonoVue microbubbles (SV) and focused ultrasound (US) on polymer coated adenovirus (PC-Ad) pharmacokinetics and tumor accumulation. **A)** The effect of focused US on the pharmacokinetics of intravenously injected 1×10^{10} copies of Ad or PC-Ad in Balbc/SCID mice bearing a ZR-75-1 xenograft tumor. Injection and US exposure regime as described in Methods. Blood was sampled 5, 15, and 30 minutes after injection, and Ad genome content was quantified by quantitative polymerase chain reaction. The enhanced circulation of PC-Ad indicates the potential for improved passive uptake into tumors. **B)** Luciferase expression in the livers of mice injected with 1×10^{10} copies of Ad or PC-Ad as analyzed 20 hours after injection by IVIS imaging. Lower expression is indicative of lower capture by the liver and lowered potential toxicity. **C)** Assay of liver damage

by quantification of ALT liver enzyme release 24 hours after injection with Ad or PC-Ad. Reduced ALT release shows PC-Ad to have reduced hepatic toxicity. **D** and **E)** The influence of focused US on tumor accumulation after intravenous delivery of Ad or PC-Ad and SV to Balbc/SCID mice bearing a ZR-75-1 xenograft on each hind leg, one of which was exposed to ultrasound, the other of which was not. Twenty hours after injection, mice were killed, and Ad genome content in tumors and liver was determined by quantitative polymerase chain reaction. Standard deviation is shown by bars. In **(A)** $n = 8$ mice, in **(B–E)** $n = 4$ mice. Analysis as done using analysis of variance with Tukey to compare all groups after test. Results are typical of two independent experiments. All statistical tests were two-sided. PBS = phosphate-buffered saline.

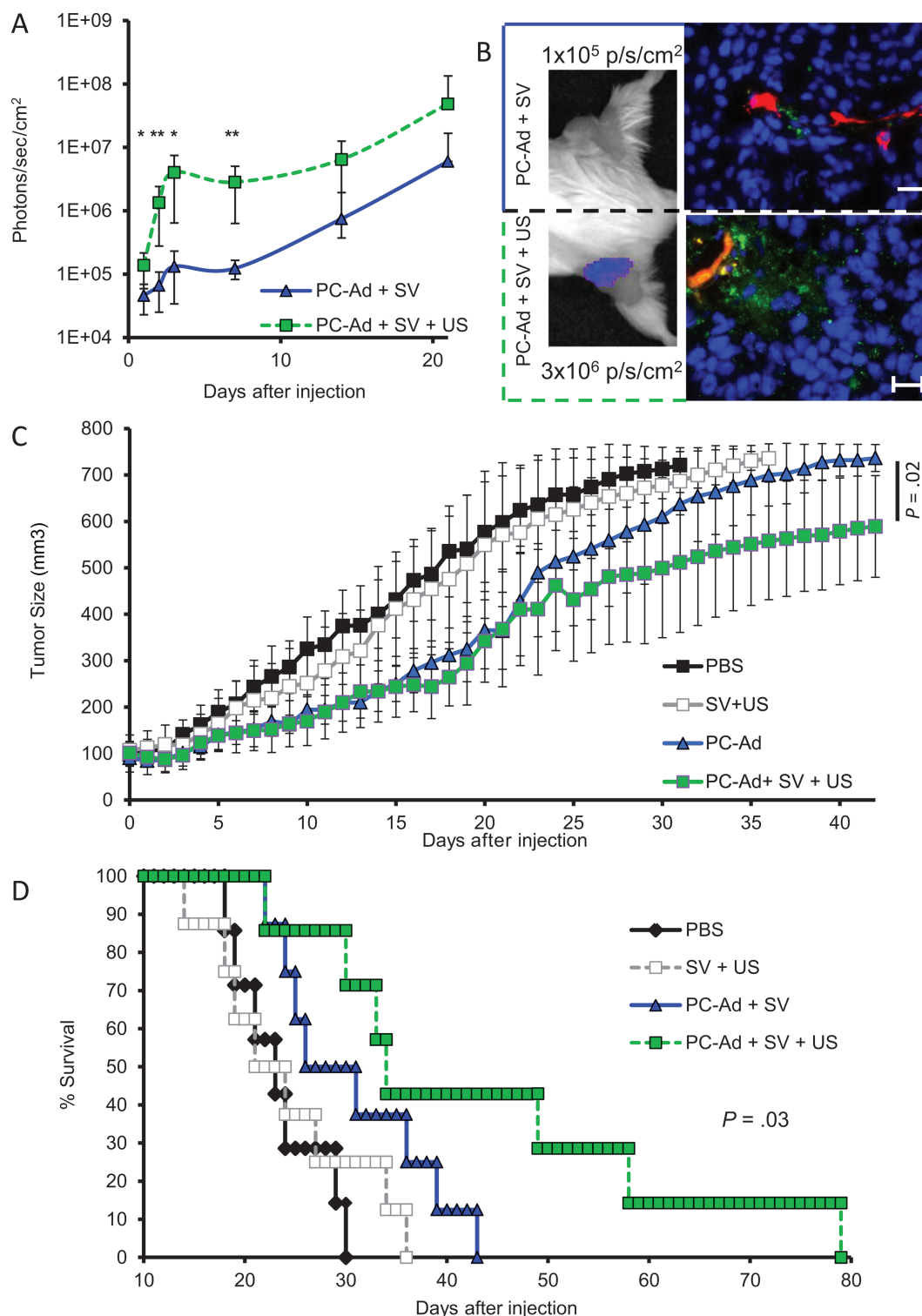


Figure 4. Transgene expression and influence on tumor growth inhibition of polymer coated adenovirus (PC-Ad) with focused ultrasound (US) in the presence of SonoVue microbubbles (SV). **A**) Luciferase transgene expression in tumors of mice injected intravenously with PC-Ad and treated simultaneously with US or not, as quantified using IVIS for the first 20 days after injection. Improved luciferase expression in US-treated tumors indicates increased replication and spread. $n = 8$. Standard deviation is shown by bars. Two-sided t test performed at each time-point. At 1, 2, 3, and 7 days, $P = .007$, $.004$, $.03$, and $.004$, respectively. **B**) Staining of tumor sections with anti-CD31 (red) or anti-hexon (green) to determine the influence of US on intratumoral penetration of PC-Ad. Scale bar = 20 µm. Staining of Ad away from

endothelial cells suggests improved penetration into tumors. **C**) Tumor growth in mice treated with phosphate-buffered saline (PBS) (black line), focused ultrasound and SV but no PC-Ad (gray line), PC-Ad with SV without focused ultrasound (blue line), or PC-Ad with SV with ultrasound (green line), as assessed by daily measurement with calipers. $n = 8$ mice. Mean values \pm 95% confidence intervals are shown. Analysis of variance with Tukey correction comparing all groups post-test was used. **D**) Kaplan-Meier survival curve of mice treated in (C), in accordance with animal welfare legislation, mice were killed when tumor size reached a predefined limit of 700 mm³. Log-rank test was performed. Results are typical of two independent experiments. All statistical tests were two-sided.

10-fold ($P = .01$) enhancement in the area under the curve of data in Figure 4A (Supplementary Figure 3A, available online). There was no weight loss or increase in ALT levels above background in any treatment group (data not shown) and no difference in hepatic luciferase levels between ultrasound-treated and non-ultrasound-treated mice (Supplementary Figure 3A, available online).

The possibility that improved intratumoral distribution permits small increases in uptake to translate into dramatic increases in infection was confirmed using fluorescence microscopy of tumor sections (Figure 4B; Supplementary Figure 3F, available online). Tumors treated with PC-Ad + SV without ultrasound (panel iv) showed staining of virus (in green) to be associated with vasculature (in red), whereas tumors treated with PC-Ad + SV + ultrasound (panel v) showed virus staining also at locations more than 100 μm from the vasculature. Analysis of multiple sections using ImageJ (<http://rsbweb.nih.gov/ij/>) software confirmed a statistically significant ($P = .04$) and substantial increase (fivefold at $<100 \mu\text{m}$ and 40-fold at $>100 \mu\text{m}$ from the vasculature) in green staining in tumors treated with PC-Ad + SV + ultrasound compared with tumors treated with PC-Ad + SV (Supplementary Figure 3G, available online). Even though this effect is probably more pronounced for a self-amplifying therapy such as virotherapy, this finding is likely to have major implications for all forms of nanotherapeutic delivery to tumors (15,16).

Tumor growth was statistically significantly retarded with PC-Ad + SV + ultrasound compared with all other treatment groups. This was the case if mean tumor sizes at day 42, PC-Ad + SV + ultrasound vs PC-Ad + SV ($P = .02$) (Figure 4C), or mean areas under the curves of tumor growth were compared (PC-Ad + SV + ultrasound; mean = 12 710 mm^3 ; SD = 3177 vs PC-Ad + SV; 18 318 mm^3 ; SD = 4665; $P = .04$) (Supplementary Figure 3A, available online) [as by (34)]. Notably, higher luciferase expression was associated with greater retardation of tumor growth and survival extension. Levels of 2×10^8 to 1×10^9 photons/sec/ cm^2 were associated with almost complete growth retardation. Kaplan–Meier analysis demonstrated median days survival values of 22 for PBS, 21 for SV + ultrasound, 26 for PC-Ad + SV = 26, and 33 for PC-Ad + SV + ultrasound (Figure 4D). By log-rank test these curves were shown to be statistically significantly different ($P = .03$). Postcull analysis showed tumors treated with PC-Ad + SV + ultrasound to have 400-fold higher luciferase and 200-fold higher virus genome content (Supplementary Fig. 3, D and E available online). This represents a million-fold increase on the tumoral PC-Ad content detected 20 hours after intravenous administration in Figure 3E. In the absence of ultrasound, PC-Ad achieved a total of approximately 5×10^7 copies/mg tumor. This matches the level previously identified as a plateau for Ad in xenograft tumours, a plateau that was reached regardless of the dose injected or whether that dose achieved anti-tumor efficacy (35), leading to the suggestion that both the initial concentration and the distribution of Ad ultimately determines the tumor control achieved. Here, we demonstrate that enhanced uptake (Figure 3F) and penetration (Figure 4B; Supplementary Figure 3F) of PC-Ad upon SV + ultrasound application provides a method of breaking through this plateau. We demonstrate the widespread intratumoral distribution achieved with PC-Ad + SV + ultrasound allows viral oncolysis to continue unhindered by spatial or resource restrictions. This allowed tumor growth retardation

to be achieved with single low-doses of virus where multiple high doses would usually be required (32).

Discussion

Treatment of metastatic cancer may require therapies that can be administered intravenously and accumulate within all disease deposits. Oncolytic viruses have the potential to powerfully and selectively kill cancer cells (36). However, in common with other macromolecular therapeutics, the intravenous delivery and antitumor activity of oncolytic viruses is limited by poor bloodstream stability, extravasation from the bloodstream into the tumor, and penetration through the tumor (4,32). The impact of these limitations is exemplified by the fact that in preclinical studies oncolytic Ads required a 1000-fold higher intravenous dose to match the efficacy of intratumoral injection (35), despite the difficulties faced in achieving consistent intratumoral injection (37). Failure to overcome these limitations has led to a lack of progress in expanding the clinical utility of Ads beyond their use in direct intratumoral delivery regimens (3).

We describe a hydrazone bond-containing copolymer that can stealth Ads, but which cleaves upon exposure to pH levels similar to those present within tumors (11). This allows efficient coating to provide blood stability and avoidance of liver capture while also enabling uncoating and reactivation for antitumor activity. Stealthing lowers liver capture/toxicity by increasing the diameter of the Ad above the size of the hepatic sinusoidal fenestrae and by lowering Kupffer cell-mediated capture (26,38). The net result was enhanced circulation, and in accordance with the enhanced permeability retention effect (13) and our own previous studies (32), this ultimately provided increased tumor accumulation (Figure 3). Notably, in common with other nanoscale therapeutics (16), enhanced permeability retention assisted accumulation of PC-Ad occurred in perivascular regions. A combination of high intratumoral pressure, lack of convective flow, and dense extracellular matrix prevents effective penetration of macromolecules from perivascular regions into and throughout the tumor (15), leading to suboptimal anti-tumor efficacy.

Ultrasound is an inexpensive, readily available modality that can achieve tissue penetration depths of 15 cm, and with novel probes and algorithms can even image through bone (39). Furthermore, ultrasound is increasingly being used as a tool to assist treatment rather than just being used for imaging. Indeed, ultrasound application in the presence of microbubbles has the potential to provide a powerful, safe stimulus for movement of a range of agents from the circulation into tumors (21). Previous studies have shown that a complement-coated Ad + microbubble formulation may provide improved tumor growth retardation compared with delivery of Ad alone (40). However, quantification and mapping of the distribution of Ad or Ad + microbubble within tumors in response to ultrasound was not reported. Furthermore, intravenous injection of Ad + microbubble into mice bearing two tumors provided no increase in the killing of the ultrasound-treated tumor compared with the contralateral non-ultrasound-treated tumor (40). Although it was suggested that a bystander immune effect led to equivalent killing of ultrasound and non-ultrasound-treated tumors, this could not be fully validated because the control, Ad + microbubble-injected mice

in which neither tumor was ultrasound treated, was not reported (40). These limitations are possibly the result of a failure to fully characterize the circulation kinetics of the formulation used or to define the ultrasound events instigated in these studies. Our previous studies using ultrasound with nonmodified Ad were limited by poor circulation kinetics and high toxicity. Hence, no ultrasound-mediated increases in tumor uptake were observed, and although enhancements in Ad tumor infection were seen, these increases were highly variable, and their effects on tumor growth could not be measured over the long term (31). Although the polymer coating employed in the studies reported here allowed these limitations to be overcome, the ultimate clinical utility of the approach may still be restricted by the requirement for the location of the cavitation agent SV to be coincident with the virus it impacts upon. Indeed a more effective nanoscale cavitation nuclei requiring less redosing than SV may have provided tumor retardation above the modest levels reported here.

However, we do demonstrate for the first time improvement to both the amount of PC-Ad entering tumors and its intratumoural penetration/distribution. Such findings have important ramifications for the efficacy of all nanoscale therapeutics, including liposomes and polymer-drug conjugates. The fact that we can instigate and concurrently detect inertial cavitation means that noninvasive feedback on the success of the procedure is possible, further improving potential clinical utility.

We show that these two different technologies are highly complementary, with polymer coating providing high circulating concentrations of PC-Ad so that ultrasound can move therapeutically useful quantities of virus beyond the perivascular space within the tumor to sites where polymer uncoating and virus replication are optimal (24). Clinically, the extended circulation of PC-Ad may allow the ultrasound exposure probe to be repositioned so that a series of preregistered tumor metastases could be treated in one session. The cancer cell selectivity of oncolytic viruses even offers the possibility of defocusing the ultrasound so that particularly florid disease could be treated. The strategy and technology we describe may ultimately improve and expand the clinical utility of these and other nanomedicines.

References

1. Khuri FR, Nemunaitis J, Ganly I, et al. A controlled trial of intratumoral ONYX-015, a selectively-replicating adenovirus, in combination with cisplatin and 5-fluorouracil in patients with recurrent head and neck cancer. *Nat Med*. 2000;6(8):879–885.
2. Liu TC, Galanis E, Kimm D. Clinical trial results with oncolytic virotherapy: a century of promise, a decade of progress. *Nat Clin Pract Oncol*. 2007;4(2):101–117.
3. Peng Z, Yu Q, Bao L. The application of gene therapy in China. *IDrugs*. 2008;11(5):346–350.
4. Carlisle RC, Di Y, Cerny AM, et al. Human erythrocytes bind and inactivate type 5 adenovirus by presenting Coxsackie virus-adenovirus receptor and complement receptor 1. *Blood*. 2009;113(9):1909–1918.
5. Lyons M, Onion D, Green NK, et al. Adenovirus type 5 interactions with human blood cells may compromise systemic delivery. *Mol Ther*. 2006;14(1):118–128.
6. Danielsson A, Elgue G, Nilsson BM, et al. An ex vivo loop system models the toxicity and efficacy of PEGylated and unmodified adenovirus serotype 5 in whole human blood. *Gene Ther*. 2010;17(6):752–762.
7. Doronin K, Shashkova EV, May SM, et al. Chemical modification with high molecular weight polyethylene glycol reduces transduction of hepatocytes and increases efficacy of intravenously delivered oncolytic adenovirus. *Hum Gene Ther*. 2009;20(9):975–988.
8. Subr V, Kostka L, Selby-Milic T, et al. Coating of adenovirus type 5 with polymers containing quaternary amines prevents binding to blood components. *J Control Release*. 2009;135(2):152–158.
9. Wonganan P, Clemens CC, Brasky K, et al. Species differences in the pharmacology and toxicology of PEGylated helper-dependent adenovirus. *Mol Pharm*. 2011;8(1):78–92.
10. Green NK, Herbert CW, Hale SJ, et al. Extended plasma circulation time and decreased toxicity of polymer-coated adenovirus. *Gene Ther*. 2004;11(16):1256–1263.
11. Vaupel P. The role of hypoxia-induced factors in tumor progression. *Oncologist*. 2004;9(Suppl 5):10–17.
12. Vaupel P, Okunieff P, Neuringer LJ. Blood flow, tissue oxygenation, pH distribution, and energy metabolism of murine mammary adenocarcinomas during growth. *Adv Exp Med Biol*. 1989;248(1):835–845.
13. Maeda H. The enhanced permeability and retention (EPR) effect in tumor vasculature: the key role of tumor-selective macromolecular drug targeting. *Adv Enzyme Regul*. 2001;41(1):189–207.
14. Chen HH, Cawood R, El-Sherbini Y, et al. Active adenoviral vascular penetration by targeted formation of heterocellular endothelial-epithelial syncytia. *Mol Ther*. 2011;19(1):67–75.
15. Magzoub M, Jin S, Verkman AS. Enhanced macromolecule diffusion deep in tumors after enzymatic digestion of extracellular matrix collagen and its associated proteoglycan decorin. *FASEB J*. 2008;22(1):276–284.
16. Tailor TD, Hanna G, Yarmolenko PS, et al. Effect of pazopanib on tumor microenvironment and liposome delivery. *Mol Cancer Ther*. 2010;9(6):1798–1808.
17. Tredan O, Galmarini CM, Patel K, et al. Drug resistance and the solid tumor microenvironment. *J Natl Cancer Inst*. 2007;99(19):1441–1454.
18. Gormley AJ, Larson N, Sadekar S, et al. Guided delivery of polymer therapeutics using plasmonic photothermal therapy. *Nano Today*. 2012;7(3):158–167.
19. Veisheh O, Gunn JW, Zhang M. Design and fabrication of magnetic nanoparticles for targeted drug delivery and imaging. *Adv Drug Deliv Rev*. 2010;62(3):284–304.
20. Rapoport N, Gao Z, Kennedy A. Multifunctional nanoparticles for combining ultrasonic tumor imaging and targeted chemotherapy. *J Natl Cancer Inst*. 2007;99(14):1095–1106.
21. Mo S, Coussios CC, Seymour L, et al. Ultrasound-enhanced drug delivery for cancer. *Expert Opin Drug Deliv*. 2012;9(12):1525–1538.
22. Bazan-Peregrino M, Arvanitis CD, Rifai B, et al. Ultrasound-induced cavitation enhances the delivery and therapeutic efficacy of an oncolytic virus in an in vitro model. *J Control Release*. 2012;157(2):235–242.
23. Arvanitis CD, Bazan-Peregrino M, Rifai B, et al. Cavitation-enhanced extravasation for drug delivery. *Ultrasound Med Biol*. 2011;37(11):1838–1852.
24. Bazan-Peregrino M, Carlisle RC, Hernandez-Alcoceba R, et al. Comparison of molecular strategies for breast cancer virotherapy using oncolytic adenovirus. *Hum Gene Ther*. 2008;19(9):873–886.
25. Ulbrich K, Subr V, Strohalm J, et al. Polymeric drugs based on conjugates of synthetic and natural macromolecules. I. Synthesis and physico-chemical characterisation. *J Control Release*. 2000;64(1–3):63–79.
26. Laga R, Carlisle R, Tangney M, et al. Polymer coatings for delivery of nucleic acid therapeutics. *J Control Release*. 2012;161(2):537–553.
27. Cichon G, Boeckh-Herwig S, Schmidt HH, et al. Complement activation by recombinant adenoviruses. *Gene Ther*. 2001;8(23):1794–1800.
28. Cotter MJ, Zaiss AK, Muruve DA. Neutrophils interact with adenovirus vectors via Fc receptors and complement receptor 1. *J Virol*. 2005;79(23):14622–14631.
29. Schnell MA, Zhang Y, Tazelaar J, et al. Activation of innate immunity in nonhuman primates following intraportal administration of adenoviral vectors. *Mol Ther*. 2001;3(5 Pt 1):708–722.
30. Miller DL, Thomas RM. Ultrasound contrast agents nucleate inertial cavitation in vitro. *Ultrasound Med Biol*. 1995;21(8):1059–1065.
31. Bazan-Peregrino M, Rifai B, Carlisle RC, et al. Cavitation-enhanced delivery of a replicating oncolytic adenovirus to tumors using focused ultrasound. *J Control Release*. 2013;169(1–2):40–47.

32. Green NK, Hale A, Cawood R, et al. Tropism ablation and stealthing of oncolytic adenovirus enhances systemic delivery to tumors and improves virotherapy of cancer. *Nanomedicine (Lond)*. 2012;7(11):1683–1695.
33. Vaupel P. Tumor microenvironmental physiology and its implications for radiation oncology. *Semin Radiat Oncol*. 2004;14(3):198–206.
34. Duan F, Simeone S, Wu R, et al. Area under the curve as a tool to measure kinetics of tumor growth in experimental animals. *J Immunol Methods*. 2012;382(1–2):224–228.
35. Demers GW, Johnson DE, Tsai V, et al. Pharmacologic indicators of antitumor efficacy for oncolytic virotherapy. *Cancer Res*. 2003;63(14):4003–4008.
36. Russell SJ, Peng KW, Bell JC. Oncolytic virotherapy. *Nat Biotechnol*. 2012;30(7):658–670.
37. Bazan-Peregrino M, Carlisle RC, Purdie L, et al. Factors influencing retention of adenovirus within tumours following direct intratumoural injection. *Gene Ther*. 2008;15(9):688–694.
38. Wisse E, Jacobs F, Topal B, et al. The size of endothelial fenestrae in human liver sinusoids: implications for hepatocyte-directed gene transfer. *Gene Ther*. 2008;15(17):1193–1199.
39. Mace E, Montaldo G, Cohen I, et al. Functional ultrasound imaging of the brain. *Nat Methods*. 2011;8(8):662–664.
40. Greco A, Di Benedetto A, Howard CM, et al. Eradication of therapy-resistant human prostate tumors using an ultrasound-guided

site-specific cancer terminator virus delivery approach. *Mol Ther*. 2010;18(2):295–306.

Funding

This work was supported by the Engineering and Physical Sciences Research Council (EPSRC) of the United Kingdom (to RC, JC, and CCC) under Challenging Engineering award EP/F011547/1; the Wellcome Trust and EPSRC under grant number WT088877/Z/09/Z (to RC); the Bellhouse Foundation and Magdalen College, Oxford UK (to MB-P); the Breast Cancer Campaign (to MB-P and LWS); and Cancer Research UK (to LWS). Praemium Academiae from Academy of Sciences of the Czech Republic (to KU, LK, VS).

Notes

We are grateful to James Fisk (University of Oxford) for manufacturing the various holders, transducer cones, and tanks used in this work.

Affiliations of authors: Institute of Biomedical Engineering, Department of Engineering Science(RC, JC, C-CC) and Department of Oncology (RL, LWS), University of Oxford, Oxford, UK; Institut d'Investigacio Biomedica de Bellvitge, L'Hospitalet de Llobregat, Barcelona, Spain (MB-P); Institute of Macromolecular Chemistry, Academy of Sciences of the Czech Republic, Prague, Czech Republic (VS, LK, KU).